Ultrafast Ring Closure Energetics and Dynamics of Cyclopentadienyl Manganese Tricarbonyl Derivatives

Tianjie Jiao,[†] Zhen Pang,[‡] Theodore J. Burkey,*[,†] Randy F. Johnston,[§] Todd A. Heimer,[¶,⊥] Valeria D. Kleiman,[¶,||] and Edwin J. Heilweil*[,¶]

Contribution from the Department of Chemistry, Campus Box 526060, The University of Memphis, Memphis, Tennessee 38152-6060, Department of Chemistry, Union University, Jackson, Tennessee 38305, and B208 Building 221, Physics Laboratory, National Institute of Standards and Technology, Gaithersburg, Maryland 20899

Received September 14, 1998

Abstract: Ring closure following flash photolysis in alkane solvents has been detected for several complexes in the series (η^5-C_5H_4R)$Mn(CO)_3$ where R = $COCH_3$ (**1**), $COCH_2SCH_3$ (**2**), $CO(CH_2)_2SCH_3$ (**3**), $COCH_2OCH_3$ (**4**), $(CH_2)_2CO_2CH_3$ (**5**), and $CH_2CO_2CH_3$ (**6**). In each case where ring closure occurs, a metal CO is ultimately substituted by the side chain functional group. Photoacoustic calorimetry studies reveal that ring closures occur with rate constants faster than 10^7 s^{-1} or between 10^6 and 10^7 s^{-1}, or in some cases the ring closure is biphasic with rate constants in both ranges. The enthalpies of CO dissociation followed by ring closure for **2** and **3** are the same (12 kcal/mol) and more favorable than those for **4**−**6** (25−15 kcal/mol). Studies of **1**−**3** by transient picosecond to microsecond infrared spectroscopy confirm biphasic dynamics for **2** and **3**: ring closure occurs immediately ($k > 5 \times 10^9$ s^{-1}) and at slower rates ($k = 10^8$−10^6 s^{-1}). We propose that some ring closure occurs before solvent coordination and that the remaining ring closure, resulting in the displacement of solvent, is much slower. The relationships of the rates and energetics of ring closure to structure and quantum yields are discussed.

Introduction

The yields of products generated from photolytic fragments can be dependent on geminate recombination or interactions with the solvent,[1,2] which often occur faster than diffusion-controlled processes.[3] In such cases efforts to change quantum yields require intervention at very short time scales. We recently succeeded in dramatically improving the quantum yields for the ligand substitution of $(C_5H_4R)Mn(CO)_3$ complexes where side chains could effectively trap the coordinatively unsaturated metal center (Scheme 1).[4] In particular, unit quantum yields for ring closure were observed in at least two cases, and require that CO recombination does not occur. The latter process has been reported to have a lifetime on the order of 300 fs for other metal carbonyls.[3] Assuming cage recombination of CO occurs, this suggests that ring closure must occur in less than 300 fs, a lifetime much shorter than those typically reported for closure of 5−6 membered rings.[5,6] Given this assumption, it was not clear why unit quantum yields were obtained in some cases and not others. To better understand how the side-chain structure affects the quantum yield for substitution, we have investigated the dynamics and energetics of ring closure of $(C_5H_4R)Mn(CO)_3$ [R = $COCH_3$ (**1**), $COCH_2SCH_3$ (**2**), $CO(CH_2)_2SCH_3$ (**3**), $COCH_2OCH_3$ (**4**), $(CH_2)_2CO_2CH_3$ (**5**), and $CH_2CO_2CH_3$ (**6**)] by using photoacoustic calorimetry (PAC) and transient infrared spectroscopy. Time-resolved studies of $CpMn(CO)_3$ have been reported previously, but only one study has examined ring closure of CpMn-type complexes.[7] In this later study, the quantum yields for ring closure were only 0.6 and independent of chain length.

Scheme 1

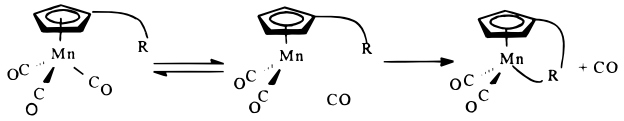

Experimental Section

Photoacoustic Calorimetry. The apparatus and methods have been described previously.[8,9] A solution in a flow cell, irradiated with a laser pulse, produces an acoustic wave that is detected as a signal from an ultrasonic transducer clamped to the cell. Ferrocene was used in

[†] The University of Memphis.
[‡] Current address, Department of Chemistry, Fudan University, China.
[§] Union University.
[¶] National Institute of Standards and Technology.
[⊥] NIST/NRC Postdoctoral Associate.
[||] Guest Researcher from UCLA Department of Chemical Engineering. Current address: Condensed Matter and Radiation Sciences Division, Naval Research Laboratory, Washington, DC 20375.

(1) Wieland, S.; van Eldik, R. *J. Phys. Chem.* **1990**, *94*, 5865.
(2) (a) Burdett, J. K.; Grzybowski, J. M.; Perutz, R. N.; Poliakoff, M.; Turner, J. J.; Turner, R. F. *Inorg. Chem.* **1978**, *17*, 147. (b) Turner, J. J.; Poliakoff, M. *ACS Symp. Ser.* **1983**, *200*, 35.
(3) (a) Kim, S. K.; Pedersen, S.; Zewail, A. H. *Chem. Phys. Lett.* **1995**, *233*, 500. (b) Schwartz, B. J.; King, J. C.; Zhang, J. Z.; Harris, C. B. *Chem. Phys. Lett.* **1993**, *203*, 503.
(4) Pang, Z.; Burkey, T. J.; Johnston, R. F. *Organometallics* **1997**, *16*, 120.
(5) (a) Winnik, M. A. *Chem. Rev.* **1981**, *81*, 491. (b) Scott, T. W.; Doubleday, C., Jr. *Chem. Phys. Lett.* **1991**, *178*, 9.
(6) For a notable exception see the following paper: Zhang, J. Z.; Schwartz, B. J.; King, J. C.; Harris, C. B. *J. Am. Chem. Soc.* **1992**, *114*, 10921.
(7) For leading references see: (a) Klassen, J. K.; Selke, M.; Sorensen, A. A.; Yang, G. K. *J. Am. Chem. Soc.* **1990**, *112*, 1267. (b) Yang, H.; Asplund, M. C.; Kotz, K. T.; Wilkens, M. J.; Frei, J.; Harris, C. B. *J. Am. Chem. Soc.* **1998**, *120*, 10154. (c) Sorenson, A. A.; Yang, G. K. *J. Am. Chem. Soc.* **1991**, *113*, 7061.

10.1021/ja9832764 CCC: $18.00
Published on Web 05/01/1999

reference solutions to provide an instrument limited signal (ca. 0.1 μs) and deposits all light energy as heat.[8,10] Sample signals were deconvoluted with the ferrocene signal by using MQP or Sound Analysis 3000 by Quantum Northwest. The deconvolution software expresses the amplitude of the sample heat decays as a fraction (ϕ) of the heat deposited by the reference solution. One or two heat decays were detected in each case. The amplitude of the first heat decay (ϕ_1) corresponds to those processes with lifetimes (τ_1) much faster than the transducer response. Heat decays for these processes cannot be resolved from each other. The amplitude of the second heat decay (ϕ_2) corresponds to processes evolving heat with lifetimes (τ_2) comparable to the transducer response. The heat evolved per mole of absorbed photons (Δ) and rate constants were calculated from eqs 1−3 where $E_{h\nu}$ is the photon energy (kcal/mol) and Φ is the net quantum yield for product formation (CO substitution by added Lewis base or side-chain substituent). The quantum yields have been reported previously.[4] The quantum yield may also correspond to the quantum yield for formation of an intermediate if the intermediate is quantitatively converted to product.[4] Each ϕ is determined by how much each process is completed during the corresponding time scale. Thus the total heat (and quantum yield) of a specific process can be assigned to Δ_1 only if the process is completed faster than the time scale of the transducer. Likewise, the assignment of the total heat (and quantum yield) of a process to Δ_2 can be made only if the process is completed on the same time scale of the transducer. Under these circumstances $\Delta = \Delta H$, the enthalpy of the process (kcal/mol). Without knowledge of the yield of a process during each time scale the heat of that process may not be calculated explicitly from ϕ_1 or ϕ_2. On the other hand, if one or more processes begin during the measurement of ϕ_1 and they are completed during the measurement of ϕ_2 then the overall heat may be calculated from eqs 1 and 2. An additional requirement for this latter case is that all intermediates lead to a final product(s) for which the quantum yield(s) of formation is known (an analytical proof is provided in the Supporting Information).

$$\Delta_1 = E_{h\nu}(1 - \phi_1)/\Phi \quad (1)$$

$$\Delta_2 = -E_{h\nu}\phi_2/\Phi \quad (2)$$

$$1/\tau_2 = k_0 + k_2[\mathrm{L}] \quad (3)$$

In a typical experiment, **1** (5.9 mg, 24 μmol) was dissolved in 50 mL of heptane in a glovebox. This solution (31.8 mL) was diluted to 200 mL with heptane to make a 0.1 OD (optical density) at 337 nm. The dilute solution was cannulated into a calibrated helium-purged reservoir with triethyl phosphate (740 μL, 4.4 mmol) to a final volume of 50 mL. The maximum laser energy was 20 μJ/pulse at 337 nm. The laser was pulsed at 1 Hz, and PAC signals were not used if pulse energies varied more than 1 μJ from an average value. Sample solutions were passed through a flow cell so that exposed solution would not be irradiated by a subsequent pulse. Signals from 1 or 0.1 MHz transducers were averaged for 16−32 shots. The values of ϕ_1, ϕ_2, and τ_2 did not change when the pulse energy was decreased by 3-fold. Lewis base concentrations were varied by at least 10-fold. All measurements were conducted at room temperature. The error limits of heat amplitudes and rate constants from PAC studies are reported as 1σ.

Transient Infrared Spectroscopy. Ultrafast infrared spectroscopy was performed using the NIST picosecond apparatus described in detail earlier.[11,12] Modifications to the pulse compressed, regeneratively amplified (20 Hz), synchronously pumped, dual dye (R6G, DCM) laser system were made for broadband, multichannel probing and transient detection using an InSb 256 × 256 infrared array camera system.[13] Time delays (picosecond to nanosecond) were obtained with a computer-controlled optical delay stage, and UV excitation was performed at 289 nm (doubled R6G laser, 2 ps instrument resolution). All measurements were made using a flowing 1 mm path-length cell with CaF_2 windows, and solute concentrations in *n*-hexane (Fisher Optima grade without any further purification or degassing) were varied (typically 2−4 mM) to yield UV optical densities near 1.0. Transient difference spectra spanning approximately 100 cm^{-1} centered around 1960 cm^{-1} were obtained by iteratively collecting probe and reference spectra with the pump on and off (4000 total laser shots) and then averaging up to five difference spectra to produce a final averaged spectrum at each time delay. Kinetic data and transient lifetimes were obtained by fitting peak intensities as a function of time delay for spectral bands that did not overlap with other IR bands. The error limits of rate constants from transient infrared studies are reported as 1σ or 10%, whichever is greater.

An electronically delayed, Q-switched excitation laser (5 ns, 266 nm, 250 μJ at 20 Hz) was employed for >5 ns time domain measurements. This laser was synchronized to the picosecond probe laser and array detection systems with a digital delay generator (Stanford Research Systems 535) which provided output triggers for the lamp, Q-switch, and InSb array controller. These pulses were synchronously delayed (up to ca. 25 ms) from the picosecond laser system master clock (20 Hz TTL count-down signals obtained from the 41 MHz acousto-optic RF oscillator). Pump−probe delay timing was adjusted by monitoring a fast photodiode which measured pump and visible probe scatter from the sample cell front window. In this fashion, pump−probe time delays could be selected spanning nanosecond to microsecond (probe arrival before or after pump), and jitter between the pump and probe pulses was determined to be less than 1 ns. While this approach is somewhat unconventional, the method provides picosecond to millisecond time-delayed transient mid-IR spectra with mOD sensitivity covering over 100 cm^{-1} in about 10 min (ca. 4000 laser shots).

Experiments were performed at 290 and 330 nm by using both a monochromator-filtered 150 Xe arc lamp and second harmonic pulses from the tunable picosecond dye laser. When the total energy absorbed by **2** in *n*-hexane was normalized for these different wavelengths, nearly identical product formation and parent loss was observed in static difference FTIR measurements. These results imply that in this spectral region the transient IR and PAC measurements are insensitive to excitation wavelength and nonlinear photolysis effects are not significant.

Molecular Mechanics. The conformational energies of **2** and **3** were optimized by using CAChe. Dihedral angles were incremented every 15° while the potential energy of the whole molecule was optimized. Conformations about two bonds were examined for **2**: the bond between the first ethanoyl carbon and the cyclopentadienyl ring carbon and the bond between the first and second carbons of the ethanoyl group. Conformations about three bonds were examined for **3**: the bond between the first propanoyl carbon and the cyclopentadienyl ring, the bond between the first and second propanoyl carbons, and the bond between the second and third propanoyl carbons.

Results

Our studies began with PAC experiments of **1** where the displacement of CO by solvent could be observed without ring closure. At THT concentrations below 0.04 M, only a single heat decay (ϕ_1) was detected following photolysis of **1**, and the amplitude of ϕ_1 was independent of THT concentration. The value reported in Table 1 for **1** and THT is an average obtained from these low concentration data. At higher THT concentrations a second heat decay (ϕ_2) was detected, and the corresponding rate constant increased with increasing THT concentration (Figure 1). Furthermore, the amplitudes of ϕ_1 and ϕ_2 were dependent on the THT concentration although the sum of

(8) Nayak, S. K.; Burkey, T. J. *Organometallics* **1991**, *10*, 3745.
(9) Leu, G.-L.; Burkey, T. J. *J. Coord. Chem.* **1995**, *34*, 87.
(10) Maciejewski, A.; Jaworska-Augustyniak, A.; Szeluga, Z.; Wojtczak, J.; Karolczak, J. *Chem. Phys. Lett.* **1988**, *153*, 227.
(11) Certain commercial equipment, instruments, or materials are identified in this paper to adequately specify the experimental procedure. In no case does such identification imply recommendation or endorsement by NIST, nor does it imply that the materials or equipment identified are necessarily the best available for the purpose.
(12) Dougherty, T. P.; Heilweil, E. J. *Opt. Lett.* **1994**, *19*, 129.
(13) Arrivo, S. M.; Kleiman, V. D.; Dougherty, T. P.; Heilweil, E. J. *Opt. Lett.* **1997**, *22*, 1488.

Table 1. PAC Data for Photolysis of (η^5-C_5H_4R)$Mn(CO)_3$ in Heptane

complex **n**	Φ^a	ϕ_1	ϕ_2	Δ_1, kcal/mol	Δ_2, kcal/mol	$10^{-6}k^b$
1 (+ THT)[c]	0.82	0.714 ± 0.007	0.196 ± 0.011	29.6 ± 1.9	−20.3 ± 1.7	2.3 ± 0.1
1 (+ THF)[c]	0.82	0.714 ± 0.019	0.091 ± 0.048	29.6 ± 2.7	−9.4 ± 5.0	0.20 ± 0.04
1 + $OP(OEt)_3$[c]		0.703 ± 0.015	0.159 ± 0.023	30.7 ± 2.4	−16.4 ± 2.6	5.3 ± 2.8
2	1.00	0.862 ± 0.030	*d*	11.7 ± 2.6	*d*	*d*
3	0.82	0.785 ± 0.014	0.098 ± 0.007	22.2 ± 2.0	−10.0 ± 1.0	1.14 ± 0.10[e]
4	0.64	0.718 ± 0.014	0.044 ± 0.006	37.4 ± 3.5	−5.8 ± 0.9	0.97 ± 0.13[e]
4	(0.82)[f]			29.2 ± 2.3	−4.6 ± 0.7	
5	1.05	0.718 ± 0.013	0.081 ± 0.010	22.8 ± 1.7	−6.5 ± 0.9	4.6 ± 0.5[e]
6	0.94[g]	0.782 ± 0.010	0.016 ± 0.006	19.7 ± 1.4	−1.4 ± 0.5	0.8 ± 0.4[e]

[a] From ref 4. [b] Units are M^{-1} s^{-1} unless otherwise noted. [c] ϕ values are extrapolated to zero Lewis base concentration, see Results; [THT] = 0−0.7 M, [THF] = 0.01−4.2 M, [$OP(OEt)_3$] = 0−0.5 M. [d] Not detected. [e] Units are s^{-1}. [f] See Discussion. [g] Total yield for all photoproducts, see ref 4.

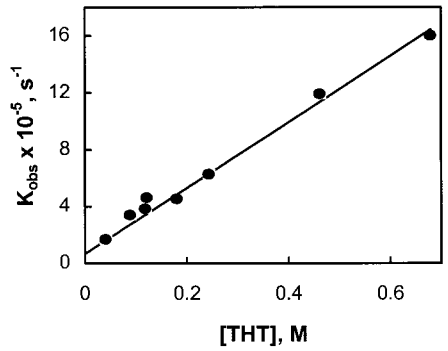

Figure 1. Plot of k_{obs} ($1/\tau_2$) versus [THT] for the second heat decay following photolysis of **1** with THT.

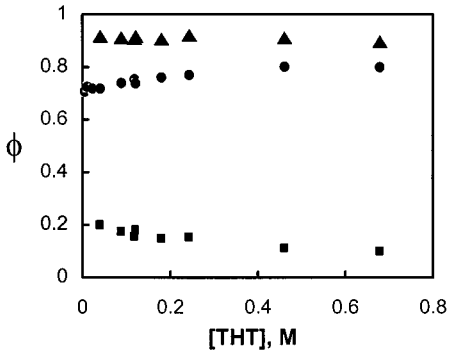

Figure 2. Heat amplitudes plotted versus THT concentration for photolysis of **1**: ▲ = $\phi_1 + \phi_2$, ● = ϕ_1, ■ = ϕ_2. The standard error is 0.03 or less, and the data markers are approximately the size of the error bars.

the amplitudes was not (Figure 2). The ϕ_2 value reported for **1** in Table 1 was obtained by subtracting the ϕ_1 value for [THT] less than 0.04 M from the averaged sum of ϕ_1 and ϕ_2 for higher [THT] (i.e., for those experiments where ϕ_2 could be detected). The ϕ_1 and ϕ_2 values reported in Table 1 are the same, within experimental error, as those obtained by extrapolating the plots in Figure 1 to zero THT concentration. Results such as those observed in Figures 1 and 2 were also obtained for **1** with THF and $OP(OEt)_3$, and the corresponding ϕ_1 and ϕ_2 were likewise calculated and reported in Table 1. At higher concentrations of $OP(OEt)_3$, saturation was observed in the kinetic data, so the rate constant was obtained at lower concentrations of $OP(OEt)_3$ where the data were linear. Two heat decays were observed for **3**−**6** but not **2** where only a fast heat decay was detected (ϕ_1).

Transient IR experiments reveal that photolysis of **1** with 0.36 M THT in *n*-hexane produces transient and product bands. The photolysis results in a partial bleach of the 1961 and 1952 cm^{-1} bands for **1**, and the amplitude of the bleach did not change during the remainder of the experiment. Two bands (**1A**) appear at 1907 and 1969 cm^{-1} within the first 200 ps after excitation.[14] These bands decay with the same rate as two new absorption bands (**1B**) grow at 1946 and 1885 cm^{-1}. The **1B** bands are stable indefinitely (monitored up to 10-μs delay). Similar results were observed following photolysis of **2** or **3** in the absence of THT, except that partial appearance of the product bands was also observed within 200 ps. For example, as shown in Figure 3, upon photolysis of **2**, there is a bleach (peaks below baseline) of parent bands at 1962 and 1953 cm^{-1} and the immediate appearance of bands at 1968, 1958, 1906 and 1898 cm^{-1}. The 1968 and 1906 cm^{-1} band intensities (**2A**) decay as the 1958 and 1898 cm^{-1} band intensities (**2B**) grow. At microsecond time delays when the 1906 cm^{-1} band of **2A** has disappeared, the intensity of the 1898 cm^{-1} band of **2B** is equal to the sum of the intensities of the 1898 and 1906 cm^{-1} bands at earlier delays. No other CO stretch IR bands are observed in this frequency range. The spectra and intensities of analogous bands for **1** and **3** behaved similarly. All spectral and kinetic data derived from transient spectra are summarized in Table 2.

Molecular mechanics calculations show that there is a considerable barrier (ca. 6 kcal/mol) to the rotation about the bond between the carbonyl carbon of the side chain and the cyclopentadienyl ring for both **2** and **3**. Thus the side chain carbonyls stay in the plane of the cyclopentadienyl ring. Only half of the conformations are discussed below and displayed in Scheme 2 since an identical set of conformations occur when the side chain carbonyls are rotated 180°. Two conformations of nearly equal energy were found for **2** where the thiomethyl group is above or below the plane of the ring. Four conformations of nearly equal energy were found for **3**, and only one of these conformations has the thiomethyl group in the proximity of the metal center.

Discussion

The results indicate that **2**−**6** undergo ring closure following photolysis, and in some cases, if not all, ring closure is biphasic. First, following CO dissociation there is an immediate ring closure that competes with solvent coordination. Second, the fraction of compound that has not immediately ring-closed subsequently closes by displacing the solvent. Before discussing the basis for these conclusions we begin with an examination of the results for **1** where ring closure was not observed.

The IR results indicate that photolysis of **1** initially dissociates CO and solvent is coordinated followed by THT displacement of coordinated solvent (Scheme 3). Thus the 1907 and 1969 cm^{-1} bands of **1A** (which decay) are assigned to (η^5-C_5H_4-$COCH_3$)$Mn(CO)_2$(hexane) by a comparison with the bands

(14) At time delays less than 200 ps the metal carbonyl molecules are still vibrationally excited and the individual IR absorbance bands are not well resolved nor reliably identified.

Table 2. Transient IR following Photolysis of $(C_5H_4R)Mn(CO)_3$ in *n*-Hexane

complex **n**	IR after 266 nm photolysis[a]				200 ps [**nB**]/[**nA**]	$10^{-6}k_{obs}$, s^{-1}	
	nA		**nB**			**nA**	**nB**
1[b]	1907	1969	1946	1885	0	2.3 ± 0.6	2.7 ± 0.7
2	1906	1968	1958	1898	1	29 ± 10	*c*
3	1907	1968	1958	1895	0.3	3.8 ± 0.8	4.3 ± 1.6

[a] ± 3 cm^{-1}; underlined bands were used for kinetic analysis, **A** is the transient and **B** is the product, see Schemes 3 and 4. [b] 0.36 M THT. [c] Not determined.

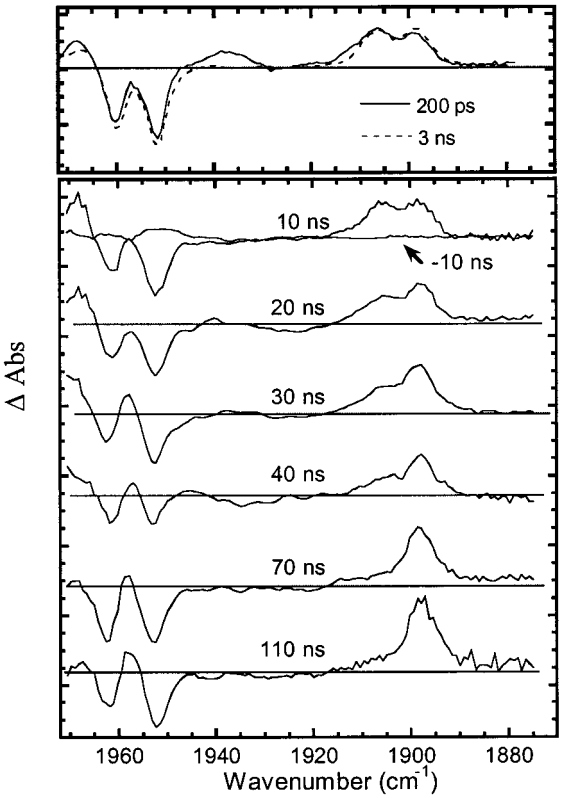

Figure 3. Transient infrared spectra of **2** in hexane.

Scheme 2

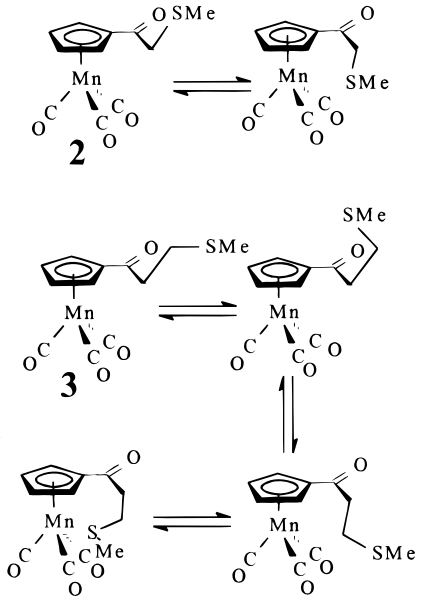

observed for $(C_5H_5)Mn(CO)_2$(heptane) (1895 and 1964 cm^{-1}),[15] and the 1946 and 1885 cm^{-1} bands of **1B** (which grow) are assigned to $(\eta^5\text{-}C_5H_4COCH_3)Mn(CO)_2$(THT) based on spectra

Scheme 3

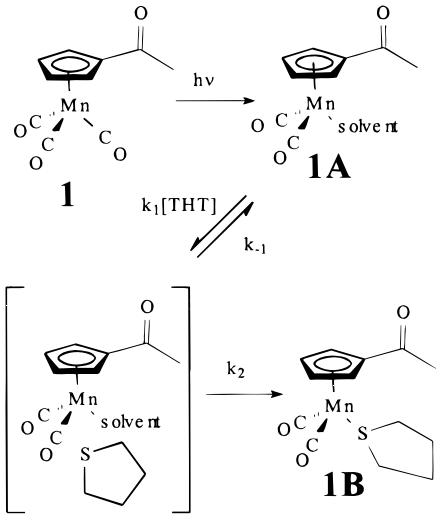

of genuine product (see Supporting Information). The assignments of ϕ_1 and ϕ_2 for photolysis of **1** are more complicated.

The changes in ϕ_1 and ϕ_2 for **1** with the concentration of THT are unusual. Typically, ϕ_1 and ϕ_2 are independent of the Lewis base concentration, and we can assign CO replacement by solvent to ϕ_1 and solvent replacement by added Lewis base to ϕ_2.[8,9] If this were the case for **1** and THT then the rate of reaction should change with THT concentration but not the extent of reaction since THT was always in large excess of the **1A** formed after each laser shot. The unusual behavior of ϕ_1 and ϕ_2 cannot be attributed to a change in the solution properties (in particular thermal expansion or polarity) for two reasons. First, the concentration of THT in the reference solution was the same as for each sample solution. As a result, the physical properties of the two solutions are the same, so deconvolution should only reveal acoustic amplitude and temporal differences due to the reactions following photolysis. Second, a change in the solvent properties would change ϕ_1 and ϕ_2 in the same direction, not opposite directions.

We surmise that ϕ_1 and ϕ_2 are not independent of each other since the sum of ϕ_1 and ϕ_2 is constant in Figure 2 as the THT concentration changes. This suggests that the same overall reaction occurs at each THT concentration, which is confirmed by the conversion of **1** to **1B** observed by transient IR experiments. The changes in ϕ_1 and ϕ_2 appear to be the result of the high concentrations of added Lewis base since the behavior was also observed for THF and $OP(OEt)_3$. The behavior of ϕ_1 and ϕ_2 is unlikely to be due to an immediate formation of an Mn−S bond in the solvent cage (which might occur at high THT concentration) since product formation was not observed in the 200 ps IR experiments. On the other hand, we cannot rule out the possibility that a THT methylene binds immediately and rearrangement to sulfur occurs on a slower

(15) Creaven, B. S.; Dixon, A. J.; Kelly, J. M.; Long, C.; Poliakoff, M. *Organometallics* **1987**, *6*, 2600.

time scale, yet if this were the case, it is difficult to explain why some Mn−S bond formation does not also immediately occur. An alternative explanation may be that a weak complex forms between **1A** and THT (Scheme 3, step 2),[16] which is consistent with the observed saturation at high THT concentration. We propose that, in addition to the displacement of CO by solvent, an interaction between **1A** and THT contributes to ϕ_1 at higher THT concentrations. If a fraction of **1A** complexes THT faster than the transducer time scale at high THT concentration then heat from this process should contribute to ϕ_1. This leaves less free **1A** to react at slower times, and the contribution to ϕ_2 of **1A** reacting with THT is less at high THT concentrations. Since the absolute change for both ϕ_1 and ϕ_2 is 0.1, we can estimate that the enthalpy of the complex formation is about 10 kcal/mol.

At a sufficiently low concentration of THT (0.04 M) with **1** the observed values for ϕ_1 and ϕ_2 are the same as those extrapolated to zero THT concentration. For these conditions, the ϕ_1 value is assigned only to solvent substitution of CO (Scheme 3, **1** to **1A**). Similarly, the ϕ_2 value is assigned to the THT substitution of solvent (Scheme 3, **1A** to **1B**).[17] This follows from the fact that the sum of ϕ_1 and ϕ_2 is constant at THT concentrations above 0.04 M and accounts for the overall conversion of **1** to **1B**. Thus subtracting ϕ_1 obtained at [THT] less than 0.04 M from the sum of ϕ_1 and ϕ_2 for [THT] obtained at greater than 0.04 M should yield a ϕ_2 (the value reported in Table 1) that corresponds only to the conversion of **1A** to **1B**. The Δ_2 calculated from this ϕ_2 is exothermic, a result that is expected for a process where the bond formed (Mn−S) is stronger than the bond broken (Mn−heptane). Finally, this assignment of ϕ_2 is consistent with (a) the dependence of the observed rate constant for ϕ_2 on THT concentration (Figure 1), (b) the change in ϕ_2 with Lewis base structure (Table 1), and (c) the similar rate constants for ϕ_2 and for the decay and growth of **1A** and **1B** IR bands, respectively (Table 2).[18]

The constant value for the sum of ϕ_1 and ϕ_2 also indicates that the quantum yield for the overall reaction must be constant (see eqs 1 and 2). At high THT concentration, occasionally THT might be expected to be in the solvent cage and react with the metal center immediately following UV photolysis. If this were the case, we would have expected the quantum yield to have increased with THT concentration. Thus the invariance of the quantum yield at the highest THT concentrations used suggests that THT does not react with the metal center prior to solvent coordination. This conclusion is confirmed by the absence of product IR bands at a 200 ps time delay (measured at 0.36 M THT).

The bimolecular rate constants for the reactions of **1A** are the slowest that have been reported for alkane solvent displacement by the ligands studied. For example, the reaction of $(C_5H_5)Mn(CO)_2$(heptane) with THF ($4.4 \pm 0.4 \times 10^6$ M^{-1} s^{-1})[19] is an order of magnitude faster than the reaction of **1A** with THF. Similarly, the rate constants for THF reaction with $W(CO)_5$(heptane) and $Mo(CO)_5$(heptane) are respectively 1 and 2 orders of magnitude larger.[20] The energetic data ($\Delta_1 + \Delta_2$) also indicate that the magnitude of Mn−L bond energies is in the order of CO > THT > $OP(OEt)_3$ > THF > heptane.

Scheme 4

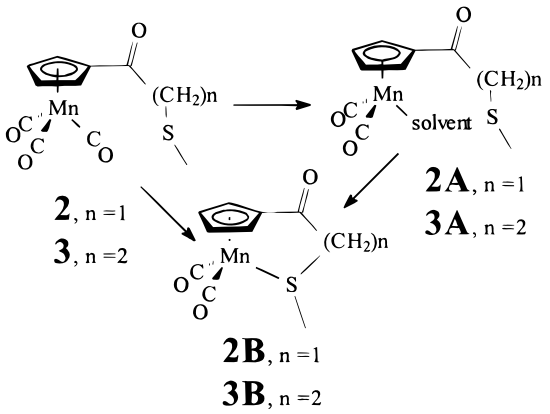

The IR experiments for **2** demonstrate that following CO dissociation both solvent-coordinated and ring-closed complexes are formed in less than 200 ps after photolysis of **2** and that the solvent-coordinated complex is converted into the ring-closed complex in about 30 ns (Scheme 4). These conclusions are based on the assignments of **2A** bands at 1906 and 1968 cm^{-1} to (η^5-$C_5H_4COCH_2SCH_3$)$Mn(CO)_2$(hexane) (by analogy to the assignments for **1A**) and the **2B** bands at 1958 and 1898 cm^{-1} to (η^6-$C_5H_4COCH_2SCH_3$)$Mn(CO)_2$ (by comparison with spectra of genuine product).[21] On the nanosecond time scale, the **2A** bands decay to the same extent that those for **2B** bands increase. Since no other bands appear we conclude that the ring closure of **2A** displaces solvent to form **2B**. The constant total intensity of the **2A** (1898 cm^{-1}) and **2B** (1906 cm^{-1}) bands implies that the peak extinction coefficients for these bands are the same. In general, the band intensities were used to calculate the ratio of product to transient species at a 200 ps delay yielding 0:1 for **1**, 1:1 for **2**, and 1:3 for **3** (see Table 2).

The total heat ($\Delta_1 + \Delta_2$) released after photolysis of **2** is the same as that for **1** reacting with THT (within experimental error) suggesting that the same overall reaction (substitution of CO by S) occurs in both PAC experiments. Since no ϕ_2 is detected for **2** and all the heat was released in a single decay (ϕ_1) we further conclude that the ring closure for **2** is much faster than the response of the PAC experiment ($k > 10^7$ s^{-1}), a conclusion consistent with the fast rate of **2B** formation observed in the IR experiments.

The results for **3** are very similar to those for **2**. The **3A** bands at 1907 and 1968 cm^{-1} are assigned to (η^5-C_5H_4CO CH_2CH_2-SCH_3)$Mn(CO)_2$(hexane) by analogy to assignments for **1A** and **2A** (Scheme 4). The **3B** bands at 1958 and 1895 cm^{-1} are assigned to (η^6-$C_5H_4COCH_2CH_2SCH_3$)$Mn(CO)_2$ by comparison with spectra of genuine product.[21] The conversion of **3A** to **3B** is about 10 times slower than the conversion of **2A** to **2B**. This is expected since the activation entropy will be greater for closing the larger ring, which has more degrees of freedom.

Two heat decays are observed after photolysis of **3** with Δ_1 and Δ_2 values between those reported for **1** and **2**. On the other hand, the sum of Δ_1 and Δ_2 is the same as those observed for **1** and **2**, suggesting that the overall reaction is the same for **1**, **2**, and **3**. The transient IR spectra at long time delays demonstrate that this reaction is CO substitution by S in each case. Since transient IR spectra indicate that **3** is converted to **3A** and **3B** within 200 ps and this is faster than the resolution

(16) We thank a reviewer for suggesting this explanation.

(17) Reaction of **1A** with unphotolyzed **1** (ca. 75 μM) is not likely to contribute to ϕ_2 since this would require a bimolecular rate constant greater than 10^{10} M^{-1} s^{-1}.

(18) In additional PAC experiments for **3** in *n*-hexane we obtained $k = (1.26 + 0.14) \times 10^6$ s^{-1}. Although the PAC and IR experiments were done in different solvents this apparently is only responsible for a minor change in the rate. Differences in rates obtained by PAC and IR experiments are attributed to the fact that IR experiments were not air free.

(19) Yang, P.-F.; Yang, G. K. *J. Am. Chem. Soc.* **1992**, *114*, 6937.

(20) Burney, D. P. Ph.D. Thesis, The University of Memphis, 1994.

(21) Pang, Z.; Johnston, R. F.; VanDerveer, D. G. *J. Organomet. Chem.* **1996**, *526*, 25.

of our PAC experiments, some ring closure must contribute to ϕ_1 (**3A** to **3B**) in addition to the contribution of CO substitution by solvent (**3** to **3A**). Consistent with this assignment of ϕ_1, the corresponding Δ_1 for **3** is more exothermic than the Δ_1 for **1** (since some Mn−S bonds have already formed for **3**) but is less exothermic than the Δ_1 for **2** (since replacement of Mn−solvent by Mn−S is not complete for **3**). The rate constant for ϕ_2 is comparable to those assigned to the decay and growth of the IR bands of **3A** and **3B**, respectively. We therefore assign this ϕ_2 to the ring closure that did not occur during the measurement of ϕ_1. Consistent with this assignment, the Δ_2 calculated from this ϕ_2 is less exothermic than that reported in Table 1 for **1**. Thus we can determine the heat of the overall reaction (**3** to **3B**) but not the heat of each reaction step (**3** to **3A** or **3A** to **3B**).

The constant values for the enthalpies of CO substitution with THT for **1** and via ring closure for **2** and **3** are not surprising considering the same types of bonds are broken and formed in each case. This comparison suggests that there is little ring strain in **2** or **3** contrary to conclusions based on spectroscopic studies.[21] The constant enthalpy also indicates that the contribution to the photoacoustic signal from the molecular volume changes during the reactions is similar for the three reactions. The reaction of **1** is an intermolecular reaction and is fundamentally different than the intramolecular reactions for **2** and **3**, and the reaction volume changes should be different. Since these differences do not significantly change the calculated overall enthalpies we conclude that the molecular volume changes make a minor contribution to the photoacoustic signal compared to that from thermal expansion. This conclusion is further supported by results for ligand substitution with $Mo(CO)_6$ where reaction volumes were shown to have an insignificant contribution to the photoacoustic signal.[22]

Conformational analysis based on molecular mechanics calculations indicates that the distribution of products 200 ps after photolysis of **2** and **3** is determined by the preferred conformations. The thiomethyl group for **2** is near the metal center 50% of the time while the thiomethyl group for **3** is near the metal center 25% of the time. This corresponds with the intensity distribution observed by transient IR (see Table 2). These results suggest that once the CO dissociates from the parent species, the metal center immediately reacts with whatever is available.

Heretofore we have assumed that the lower quantum yield for **3** compared to **2** was due to CO recombination for **3**. If this were the case the above conformational analysis does not account for nearly 20% of **3** that is reformed. In other words, assuming every photon leads to CO dissociation the distribution following photolysis would actually be 1:3:1 for **3**:**3A**:**3B**. If on the other hand no geminate recombination occurs, the conformational analysis is entirely consistent with the transient IR results. This would require that the lower quantum yield for **3** be due to excited-state deactivation. While the structures of **2** and **3** are quite similar, the proximity of sulfur to the metal center and/or the cyclopentadienyl ring in **2** may perturb the electronic structure sufficiently to make deactivation of the excited state too slow to compete with CO dissociation.

Once solvent coordination occurs, displacement of solvent by CO is slow and is governed largely by the rate of solvent dissociation.[23] Thus solvent coordination forces CO to diffuse out of the solvent cage. The displacement of solvent by CO must now compete with the "slow ring closure". Even if all of the complex were photolyzed the concentration of CO would be no more than 4 mM, and the first-order rate constant will only be about 10^3 s^{-1}. This cannot compete with the slow (10^6 s^{-1}) ring closure of **3**. Even if CO reenters the solvent cage for a secondary geminate recombination it is still destined to diffuse away.[24] We conclude that nongeminate recombination of CO cannot compete with ring closure of **2** or **3**.

Examination of PAC data for **4** suggests that the quantum yield we previously reported for **4** may be in error and should be investigated further. Two results for **4** are inconsistent with those of the other complexes. First, the structure of **4** is similar to **1** and **3** yet the quantum yield for **4** is different. Second, and more significant, the Δ_1 for **4** is much more endothermic than the Δ_1 for **1**. Ring closure, if it occurs, would make Δ_1 for **4** more exothermic than for **1** not less. If no ring closure occurs for **4**, Δ_1 should be the same for **1** since the Mn−CO bond and Mn−solvent bond strengths should be similar in both cases. Indeed, if we assume the quantum yield for **4** is the same as it is for **1** and **3** then the Δ_1 for **4** is the same as it is for **1** (see second entry for **4** in Table 1). With this assumption, the results suggest that no ring closure occurs for **4** during the first heat decay, or if it does, the enthalpy of ring closure is the same as for solvent coordination. The latter possibility is inconsistent with the exothermic second heat decay observed for **4** and for **1** with THF. We conclude that the lower limit of the quantum yield for **4** is 0.82.

The second heat decay for **4** is most likely due to ring closure by analogy to the results for **2** and **3**. This ring closure is slower than that for **2** even though the number of ring atoms in each case is the same. The shorter bond lengths associated with oxygen versus sulfur probably result in a ring strain that increases the barrier to ring closure.

By analogy to the other complexes, ring closure is expected to be biphasic for **5** and **6.** Indeed a second heat decay is observed in each case. The overall enthalpy ($\Delta_1 + \Delta_2$) for **5** is the same as for **6** and suggests that the overall reaction is the same. We assign this reaction to CO dissociation followed by ring closure. The difference in Δ_1 (and Δ_2) for the two complexes is most likely due to different extents of ring-closed product and solvent-coordinated intermediate forming immediately after CO dissociation. The overall enthalpies for **5** and **6** may be expected to be similar since both complexes have an ester function on the side chain. On the other hand, the enthalpies for **5** and **6** are less exothermic than those for **2** and **3**. This is consistent with the results for **1** with THT and THF, which show that the Mn−S bond is stronger than the analogous Mn−O bond.

Summary

Results of PAC, transient IR, and molecular mechanics studies indicate that ring closure following photolysis of (η^5-C_5H_4R)-$Mn(CO)_3$ complexes can be extremely fast; in addition, the ring closures can occur via two pathways of distinct time scales. The first pathway is an ultrafast ring closure following CO dissociation that occurs prior to solvent coordination. The second pathway is a nanosecond to microsecond ring closure that displaces coordinated solvent. Rapid ring closure following photolysis is determined by favorable side-chain conformations.

Acknowledgment. The donors of the Petroleum Research Fund, administered by the American Chemical Society, the National Science Foundation through the Academic Research

(22) Jiao, T.; Leu, G. L.; Farrell, G.; Burkey, T. J. Unpublished results.

(23) $k = 3 \times 10^5$ M^{-1} s^{-1} for R = H, and our data show that rates are even slower for solvent displacement for R = $COCH_3$, see ref 15.

(24) For further discussion of the fate of caged CO see refs 3 and 8.

Infrastructure program (STI-9602656) and a University of Memphis Faculty Research Grant are acknowledged for partial support of this research.

Supporting Information Available: The source of reagents, descriptions of the syntheses of **1**, **1B**, **2**, and **3**, an analysis of PAC heat decays, and tables of PAC data for **1**−**6** (PDF). This material is available free of charge via the Internet at http://pubs.acs.org.

JA9832764